A quantum spin approach to histone dynamics

C. Gils,[1] J. L. Wrana,[1,2] and W. K. Abou Salem[3,4]

[1]*Samuel Lunenfeld Research Institute, Mount Sinai Hospital, 600 University Ave, Toronto, ON M5G 1X5, Canada*
[2]*Department of Molecular Genetics, University of Toronto, 1 Kings College Circle, Room 4396, Toronto, ON M5S 1A8, Canada*
[3]*Department of Mathematics, University of British Columbia, 1984 Mathematics Road, Vancouver, BC V6T 1Z2, Canada*
[4]*Department of Mathematics and Statistics, University of Saskatchewan, Saskatoon, SK S7N 5E6, Canada*

(Dated: September 14, 2010)

Post-translational modifications of histone proteins are an important factor in epigenetic control that serve to regulate transcription, depending on the particular modification states of the histone proteins. We study the stochastic dynamics of histone protein states, taking into account a feedback mechanism where modified nucleosomes recruit enzymes that diffuse to adjacent nucleosomes. We map the system onto a quantum spin system whose dynamics is generated by a non-Hermitian Hamiltonian. Making an ansatz for the solution as a tensor product state leads to nonlinear partial differential equations that describe the dynamics of the system. Multiple stable histone states appear in a parameter regime whose size increases with increasing number of modification sites. We discuss the role of the spatial dependance, and we consider the effects of spatially heterogeneous enzymatic activity. Finally, we consider multistability in a model of several types of correlated post-translational modifications.

PACS numbers:

arXiv:0912.4465v2 [q-bio.MN] 12 Sep 2010

I. INTRODUCTION

Nuclear chromosomes in eukaryotic organisms consist of the chromatin, a complex wrap that is primarily composed of DNA and histone proteins. The fundamental unit of the chromatin is the nucleosome, each of which contains two copies of the core histones H2A, H2B, H3 and H4, and approximately 150 base pairs of DNA. Each of the core histone proteins exhibits multiple amino acid residues that are subject to post-translational modifications (PTM) by chemical groups such as phospho-, acetyl-, methyl- or ubiquitin-groups that can be added and removed in a reversible manner. For example, H4 has a phosphorylation site, four acetylation sites and six methylation sites. Depending on the particular modification state of histones, certain regions of DNA in the chromatin are in an active or repressed state. Regulation of the PTMs of histones lies at the center of epigenetic control [1–3].

A commonly observed epigenetic phenomenon is the existence of alternative regulatory states. For example, in the fission yeast Schizosaccharomyces pombe the two mating type cassettes, mat2-P and mat3-M are usually in a silenced state in which the mating type genes are not expressed. When removing a portion of the silenced region and inserting a ura4+ reporter gene, the expression of ura4+ and the mating-type genes becomes bistable, with a state where ura4+ is repressed and a state where ura4+ is expressed [4–6]. The silenced state of ura4+ is associated with a high concentration of methylation marks on lysine of histone H3 (H3K9), while the active ura4+ state does not exhibit methylation of H3K9 [7]. Each of the two epigenetic states is preserved under cell divisions, with transitions between them occuring only at a very low rate.

Post-translational modifications are regulated by various enzymes. In order to explain the appearance of multiple stable histone states, a non-local positive feedback mechanism has been put forward [8, 9]: A nucleosome that exhibits a particular modification recruits the enzymes that catalyze this modification. These enzymes then move to adjacent nucleosomes and cause the modification to be added there, a mechanism that has indeed been observed for some histone acetyltransferases, histone decacetylases and histone methyltransferases [10–13]. Long-range feedback has been implemented in a stochastic simulation of a three-state model (unmodified state, acetylated state, methylated state) and it was shown to lead to robust bistability [14]. Nearest-neighbour feedback has been considered in deterministic descriptions of two- and three-state models [15, 17]. The authors of Ref. [15] consider a two-state mean-field [16] description that takes into account cooperativity in binding of enzymes, and they discuss the bifurcation diagram, including the effects of spatial dependence. In Ref. [17], the results of a stochastic simulation are compared to those of a mean-field description that does not explicitly consider spatial dependence. Perturbations due to cell divisions were considered, and instability of stable steady states due to such perturbations were found in the stochastic simulation, but not the mean-field approach. It is an open question how to obtain mean-field equations in the continuum starting from a stochastic description that predict the instabilities due to spatial dependance that are observed in the microscopic simulations. Among other things, this is one of the questions that we address in this work.

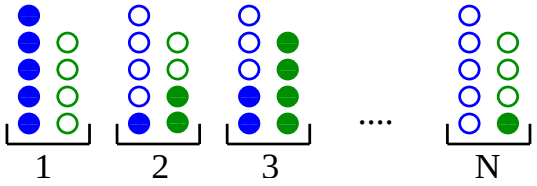

FIG. 1: Schematic illustration of an array of N nucleosomes, each of which contains $S^A = 5$ PTMs A (blue) and $S^M = 4$ PTMs M (green) where PTMs of types A are regulated by a certain set of enzymes and PTMs M are regulated by another set of enzymes. Filled circles symbolize the presence of a PTM, empty circles indicate the absence of a PTM. In this example, occupations are $n_1^A = 5$, $n_1^M = 0$, $n_2^A = 1$, $n_2^M = 2$, etc.

The considerable number of independently regulated modification sites in the chromatin has been hypothesized to give rise to a "histone code" [18]: There are 2^T possible combinations of modified/unmodified configurations of T independently regulated PTMs, each of which potentially corresponds to a distinct "read-out" of information and ultimately a different epigenetic outcome. Recent efforts in identifying abundances of these histone modification states (also denoted as histone isoforms) have revealed that only few of the large number of possible isoforms are actually observed [19, 20]. It is also well known that regulation of different PTMs is correlated. For example, phosphorylation of H3 Ser10 stimulates acetylation of H3 Lys14 [21], and methylation of H3 Lys4 and Lys79 requires the ubiquitiniation of H2B Lys123 [22, 23]. In this work, we consider how such correlations in the regulation of PTMs reduce the information capacity of histone states. In particular, we study a model that is motivated by an interaction in the H3 N terminus where Ser10 phosphorylation inhibits Lys9 methylation [24].

We consider a master equation description of the stochastic dynamics of histone states (section II). The system consists of a large number of nucleosomes, where each nucleosome exhibits several PTMs that are regulated by a particular class of enzymes. We take into account the reversible addition and removal of PTMs due to enzymatic activity, as well as on-site ("local") and nearest-neighbour ("non-local") feedback mechanisms where modified nucleosomes recruit enzymes that either act locally or diffuse to adjacent nucleosomes. We use a quantum many-body formulation of the master equation à la Doi[25] and a tensor product state ansatz to obtain a system of nonlinear difference equations (section III). We believe that the continuum limit of these equations is a suitable mean-field description that captures the role of spatial dependance in the master equation. The reader who is not interested in the derivation of the nonlinear difference equations/partial differential equations can go directly to Eqs. (10), Eqs. (13) and Eqs. (20). We numerically study the system of nonlinear partial differential equations (section IV). When considering one type of post-translational modification, and including at least two modification sites, bistable steady states are obtained without the necessity of explicit cooperativity at the level of the stochastic description (section IV A). The two stable steady states correspond to an unmodified state and a state with a high number of PTMs. We observe that increasing the number of modification sites increases the size of the parameter regime where bistable steady states exist. For a large number of modification sites, bistability is possible even if the coupling strength of the feedback mechanism is weak compared to the coupling strength of local processes. We observe that the spatial dependance due to the non-local feedback mechanism leads to instabilities of steady states under certain spatial perturbations of the histone state (section IV B). These instabilities manifest themselves in traveling wave solutions of the system of nonlinear partial differential equations. We also consider spatially dependent rate parameters, which arise from adaptor proteins, such as DNA binding transcription factors, that recruit histone modifying enzymes to specific regions of chromatin (section IV C). We discuss how such spatially dependent enzyme activity gives rise to spatial heterogeneity in the epigenetic state. Finally, we introduce a model of two types PTMs that are regulated by different classes of enzymes and mutually inhibit each other (section IV D). Such mechanisms are present in the chromatin, for example, in the case of H3 Ser10 phosphorylation that inhibits H3 Lys9 methylation [24]. We find that inhibition in one direction is sufficient to reduce the full combinatorial set of four stable steady states to a set of three stable steady states where the presence of the two types of PTM is mutually exclusive. We conclude by discussing open problems and future directions.

II. STOCHASTIC DYNAMICS OF HISTONE STATES

We consider a one-dimensional array of N nucleosomes. Each nucleosome contains several modification sites of one or several independently regulated classes of PTMs, as schematically illustrated in Fig 1. A system comprised of N nucleosomes with S^A modification sites of type A (e.g., acetylation) on each nucleosome is described by a state $|n_1^A, n_2^A, ..., n_N^A\rangle$ where the number of modified (e.g., acetylated) sites on nucleosome i is given by $n_i^A \in \{0, 1, ..., S^A\}$.

We denote by $P(n_1^A, n_2^A, ..., n_N^A; t)$ the probability of finding the system in state $|n_1^A, n_2^A, ..., n_N^A\rangle$ at time t. In this and the following sections, we shall restrict ourselves to a single class of PTMs (i.e., regulated by a particular set of enzymes); however, in section IV D we shall discuss the case of two types of PTM.

In the description of the stochastic dynamics of the histone state, we consider on-site ("local") and nearest-neighbour ("non-local") processes:

1. The addition of a PTM A at nucleosome i with a rate λ^A,

$$n_i^A \xrightarrow{\lambda^A} n_i^A + 1,$$

caused by enzymatic activity.

2. The removal of a PTM A at nucleosome i with a rate $\mu^A n_i^A$,

$$n_i^A \xrightarrow{\mu^A n_i^A} n_i^A - 1,$$

as a result of enzymatic activity.

3. The addition of a PTM A at nucleosome i with a rate $f(n_{i-1}^A, n_i^A, n_{i+1}^A)$,

$$n_i^A \xrightarrow{f(n_{i-1}^A, n_i^A, n_{i+1}^A)} n_i^A + 1.$$

The choice

$$f(n_{i-1}^A, n_i^A, n_{i+1}^A) = \tilde{\alpha}^A n_i^A + \alpha^A (n_{i-1}^A + n_{i+1}^A - 2n_i^A), \tag{1}$$

corresponds to a feedback mechanism that is both local and non-local. The first term (coupling parameter $\tilde{\alpha}^A$) accounts for local feedback: the more PTMs are present at nucleosome i, the more enzymes that add PTMs of type A (e.g., acetylases) are present at i, and the more likely is the addition of further PTMs of type A. The second term (coupling parameter α^A) corresponds to non-local feedback: the enzymes at nearest-neighbouring nucleosomes $i-1$ and $i+1$ diffuse to nucleosome i and vice versa and, as in the case of local feedback, make the addition of additional PTMs more likely.

4. The removal of a PTM A at nucleosome i with a rate $n_i^A g(n_{i-1}^A, n_i^A, n_{i+1}^A)$, i.e.,

$$n_i^A \xrightarrow{n_i^A g(n_{i-1}^A, n_i^A, n_{i+1}^A)} n_i^A - 1.$$

The choice

$$g(n_{i-1}^A, n_i^A, n_{i+1}^A) = \tilde{\beta}^A (S^A - n_i^A) + \beta^A (2n_i^A - n_{i-1}^A - n_{i+1}^A), \tag{2}$$

corresponds to a feedback mechanism that is both local and non-local. The first term (coupling parameter $\tilde{\beta}^A$) accounts for local feedback: The fewer PTMs are present at nucleosome i (i.e., the larger $S - n_i^A$), the more enzymes that cause the removal of PTM A (e.g., deacetylases) are present at i, making the removal of further PTMs more likely. The second term (coupling parameter β^A) corresponds to non-local feedback: the enzymes that cause the removal of PTMs A at nearest-neighbouring nucleosomes $i-1$ and $i+1$ diffuse to nucleosome i and vice versa and, as in the case of local feedback, make the removal of PTMs at site i more likely.

The master equation for the above processes is given by

$$\frac{dP(n_1^A, ..., n_N^A; t)}{dt} = \sum_{i=1}^{N} [\lambda^A + f(n_{i-1}^A, n_i^A, n_{i+1}^A)][P(n_1^A, ..., n_{i-1}^A, n_i^A - 1, n_{i+1}^A, ..., n_N^A; t) - P(n_1^A, ..., n_{i-1}^A, n_i^A, n_{i+1}^A, ..., n_N^A; t)]$$

$$+ \sum_{i=1}^{N} [\mu^A + g(n_{i-1}^A, n_i^A, n_{i+1}^A)][(n_i^A + 1)P(n_1^A, ..., n_{i-1}^A, n_i^A + 1, n_{i+1}^A, ..., n_N^A; t) - n_i^A P(n_1^A, ..., n_{i-1}^A, n_i^A, n_{i+1}^A, ..., n_N^A; t)]. \tag{3}$$

III. DERIVATION OF NONLINEAR DIFFERENCE EQUATIONS

We shall now introduce a notation of the master equation (3) that is motivated by quantum physics [25, 26]. Standard quantum physics notation is used, i.e., $|n_1^A, ..., n_N^A\rangle = |n_1^A\rangle \otimes |n_2^A\rangle \otimes ... \otimes |n_N^A\rangle$. We define

$$|\Psi(t)\rangle = \sum_{\{n\}} P(n_1^A, n_2^A, ..., n_N^A; t)|n_1^A, n_2^A, ..., n_N^A\rangle,$$

where the sum runs over all possible states. We introduce local raising and lowering operators [27] $\mathcal{R}_i$ and $\mathcal{L}_i$ that are defined by

$$\mathcal{L}_i^A|n_i^A\rangle = n_i^A|n_i^A - 1\rangle, \qquad \mathcal{R}_i^A|n_i^A\rangle = |n_i^A + 1\rangle, \qquad \mathcal{R}_i^A|S_i^A\rangle = 0, \qquad \mathcal{L}_i^A|0_i^A\rangle = 0,$$

Indices A and i of operators signify that the operators are applied to state $|n_i^A\rangle$. When representing states $|0^A\rangle$, $|1^A\rangle$,..., $|S^A\rangle$ by the $S^A + 1$ unit vectors in $S^A + 1$ dimensions, the lowering and raising operators can be represented by $(S^A + 1) \times (S^A + 1)$ dimensional matrices,

$$\mathcal{L}_i^A = \begin{pmatrix} 0 & 1 & 0 & ... & ... & 0 \\ 0 & 0 & 2 & 0 & ... & 0 \\ 0 & 0 & 0 & 3 & ... & 0 \\ ... & ... & ... & ... & ... & ... \\ 0 & 0 & ... & ... & ... & S^A \\ 0 & 0 & ... & ... & 0 & 0 \end{pmatrix}, \qquad \mathcal{R}_i^A = \begin{pmatrix} 0 & 0 & ... & ... & 0 & 0 \\ 1 & 0 & ... & ... & ... & 0 \\ 0 & 1 & 0 & ... & ... & 0 \\ ... & ... & ... & ... & ... & ... \\ 0 & 0 & ... & 1 & ... & ... \\ 0 & 0 & ... & ... & 1 & 0 \end{pmatrix}.$$

The number operator is defined by $\mathcal{N}_i^A = \mathcal{R}_i^A\mathcal{L}_i^A = \mathrm{Diag}(0, 1, 2, ..., S^A)$. In this notation, the master equation becomes

$$\frac{\partial|\Psi(t)\rangle}{\partial t} = \mathcal{H}|\Psi(t)\rangle, \tag{4}$$

where $\mathcal{H} = \mathcal{H}_1^A \otimes \mathcal{E}_2^A \otimes ... \otimes \mathcal{E}_N^A + \mathcal{E}_1^A \otimes \mathcal{H}_2^A \otimes ... \otimes \mathcal{E}_N^A + ... + \mathcal{E}_1^A \otimes ... \otimes \mathcal{H}_N^A$ (in simplified notation: $\mathcal{H} = \sum_{i=1}^N \mathcal{H}_i^A$), where $\mathcal{E}_i^A$ denotes the S^A-dimensional identity operator, and

$$\begin{aligned} \mathcal{H}_i^A \;=\; & \lambda^A(\mathcal{R}_i^A - \mathcal{I}_i^A) + \mu^A(\mathcal{L}_i^A - \mathcal{N}_i^A) + (\mathcal{R}_i^A - \mathcal{I}_i^A)[\alpha^A(\mathcal{N}_{i-1}^A + \mathcal{N}_{i+1}^A - 2\mathcal{N}_i^A) + \tilde{\alpha}^A\mathcal{N}_i^A] \\ & +(\mathcal{L}_i^A - \mathcal{N}_i^A)[\beta^A(\mathcal{M}_{i-1}^A + \mathcal{M}_{i+1}^A - 2\mathcal{M}_i^A) + \tilde{\beta}^A\mathcal{M}_i^A], \end{aligned} \tag{5}$$

where $\mathcal{I}^A = \mathrm{Diag}(1, 1, ..., 1, 0)$, and $\mathcal{M}^A = \mathrm{Diag}(S^A, S^A - 1, ..., 1, 0)$. In (5), we substituted the functions (1) and (2). We note that (4) is an imaginary-time Schrödinger equation. The system corresponds to a quantum spin chain, though with a non-hermitian Hamitonian.

The master equation (4) is equivalent to a functional variation [28],

$$\frac{\delta\Gamma}{\delta\Phi} = 0, \tag{6}$$

where

$$\Gamma = \int dt\langle\Phi|(\partial_t - \mathcal{H})|\Psi\rangle.$$

Since the system can be viewed as a quantum spin chain, albeit with a non-hermitian Hamiltonian $\mathcal{H}$, we make an ansatz for the wave-function in the Schrödinger picture as a tensor product state,

$$|\Psi(t)\rangle = \prod_{i=1}^N |\Psi_i(t)\rangle, \qquad \langle\Phi| = \prod_{i=1}^N \langle\Phi_i| \; . \tag{7}$$

and we write $|\Psi_i(t)\rangle$ as a superposition of all possible states (we shall drop indices A from this point on),

$$|\Psi_i(t)\rangle = \sum_{n=0}^S C_{i,n}(t)|n\rangle = \begin{pmatrix} C_{i,0}(t) \\ C_{i,1}(t) \\ . \\ . \\ . \\ C_{i,S}(t) \end{pmatrix}, \qquad \langle\Phi_i| = \sum_{n=0}^S \langle n|e^{\phi_{i,n}} = (e^{\phi_{i,0}} \;\; e^{\phi_{i,1}} \;\; ... \;\; e^{\phi_{i,S}}), \tag{8}$$

where $\sum_{n=0}^{S} C_{i,n} = 1$, and $C_{i,n}$ denotes the probability that nucleosome i has n modified sites. Since $\sum_{n=0}^{S} C_{i,n} = 1$, this ansatz obeys the probabilistic constraint $\langle\Phi|\Psi\rangle|_{\phi_{i,n}=0} = 1$ (i.e., expectation values $\langle\Phi|O|\Psi\rangle$ of an observable O are properly normalized).

Using this ansatz, the master equation in the formulation of (6) becomes

$$\left(\left\langle \frac{\partial\Phi}{\partial\phi_{i,k}}\middle|\,\frac{\partial\Psi}{\partial C_{i,n}}\right\rangle \frac{dC_{i,n}}{dt} - \left\langle \frac{\partial\Phi}{\partial\phi_{i,k}}\,|\mathcal{H}|\,\Psi\right\rangle\right)_{\phi_{i,k=0}} = 0. \tag{9}$$

Evaluating (9) yields a system of nonlinear difference equations for the probabilities $C_{i,n}$ that the nucleosome i has n modifications,

$$\begin{aligned}
\frac{dC_{i,0}}{dt} &= -\lambda C_{i,0} + \mu C_{i,1} - C_{i,0}(\alpha F_i^{\nabla} + \tilde{\alpha}\langle n_i\rangle) + C_{i,1}(\beta G_i^{\nabla} + \tilde{\beta}\langle m_i\rangle),\\
\frac{dC_{i,n}}{dt} &\overset{1\le n<S}{=} -\lambda(C_{i,n} - C_{i,n-1}) - \mu(nC_{i,n} - (n+1)C_{i,n+1}) - (C_{i,n} - C_{i,n-1})(\alpha F_i^{\nabla} + \tilde{\alpha}\langle n_i\rangle)\\
&\quad -(nC_{i,n} - (n+1)C_{i,n+1})(\beta G_i^{\nabla} + \tilde{\beta}\langle m_i\rangle),\\
\frac{dC_{i,S}}{dt} &= \lambda C_{i,S-1} - S\mu C_{i,S} + C_{i,S-1}(\alpha F_i^{\nabla} + \tilde{\alpha}\langle n_i\rangle) - SC_{i,S}(\beta G_i^{\nabla} + \tilde{\beta}\langle m_i\rangle),
\end{aligned} \tag{10}$$

where

$$\begin{aligned}
&F_i^{\nabla} = \langle n_{i-1}\rangle - 2\langle n_i\rangle + \langle n_{i+1}\rangle \quad \text{if} \quad 1 < i < N, \qquad F_1^{\nabla} = -2\langle n_1\rangle + \langle n_2\rangle \qquad F_N^{\nabla} = \langle n_{N-1}\rangle - 2\langle n_N\rangle,\\
&G_i^{\nabla} = \langle m_{i-1}\rangle - 2\langle m_i\rangle + \langle m_{i+1}\rangle \quad \text{if} \quad 1 < i < N, \qquad G_1^{\nabla} = -2\langle m_1\rangle + \langle m_2\rangle \qquad G_N^{\nabla} = \langle m_{N-1}\rangle - 2\langle m_N\rangle,
\end{aligned}$$

and

$$\langle n_i\rangle = \sum_{n=0}^{S} nC_{i,n} \tag{11}$$

$$\langle m_i\rangle = \sum_{n=0}^{S} (S-n)C_{i,n} = S - \langle n_i\rangle, \tag{12}$$

(open boundary conditions).

Equations (10) are a discretization of a system of nonlinear reaction-diffusion equations. Let ℓ_0 be the lattice spacing (distance between nucleosomes). In the mean-field/continuum limit $\alpha \to \alpha/\ell_0^2$, $\beta \to \beta/\ell_0^2$, and $\ell_0 \to 0$, we obtain the system of nonlinear partial differential equations for variables $C_n(x,t)$, $n = 0, 1, ..., S$,

$$\begin{aligned}
\frac{\partial C_0}{\partial t} &= -\lambda C_0 + \mu C_1 - C_0\left(\alpha\sum_{s=0}^{S}\left(s\frac{\partial^2 C_s}{\partial x^2}\right) + \tilde{\alpha}\sum_{s=0}^{S}(sC_s)\right) + C_1\left(\beta\sum_{s=0}^{S}\left((S-s)\frac{\partial^2 C_s}{\partial x^2}\right) + \tilde{\beta}\sum_{s=0}^{S}(S-sC_s)\right),\\
\frac{\partial C_n}{\partial t} &\overset{1\le n<S}{=} -\lambda(C_n - C_{n-1}) - \mu(nC_n - (n+1)C_{n+1}) - (C_n - C_{n-1})\left(\alpha\sum_{s=0}^{S}\left(s\frac{\partial^2 C_s}{\partial x^2}\right) + \tilde{\alpha}\sum_{s=0}^{S}(sC_s)\right)\\
&\quad -(nC_n - (n+1)C_{n+1})\left(\beta\sum_{s=0}^{S}\left((S-s)\frac{\partial^2 C_s}{\partial x^2}\right) + \tilde{\beta}\sum_{s=0}^{S}(S-sC_s)\right)\\
\frac{\partial C_S}{\partial t} &= \lambda C_{S-1} - S\mu C_S + C_{S-1}\left(\alpha\sum_{s=0}^{S}\left(s\frac{\partial^2 C_s}{\partial x^2}\right) + \tilde{\alpha}\sum_{s=0}^{S}(sC_s)\right) - SC_S\left(\beta\sum_{s=0}^{S}\left((S-s)\frac{\partial^2 C_s}{\partial x^2}\right) + \tilde{\beta}\sum_{s=0}^{S}(S-sC_s)\right).
\end{aligned} \tag{13}$$

The diffusion terms are multiplied with the probabilities themselves. We note that the coefficient in front of the diffusion term is degenerate, and it is of interest to rigorously show the existence and stability of traveling wave solutions in reaction-diffusion equations of this type.

IV. RESULTS

In what follows, our analysis is based on numerical analysis of the system (10) over a finite parameter range. In the following, we set parameters $\tilde{\alpha} = 4\alpha$ and $\tilde{\beta} = 4\beta$, and we emphasize that varying the relative strength of local and

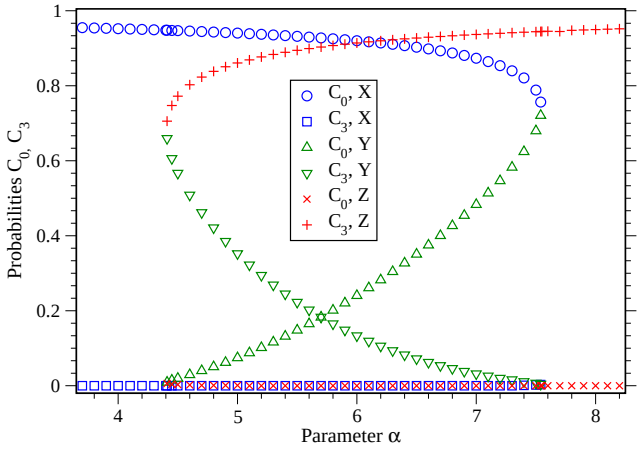

FIG. 2: Bifurcation diagram showing the steady state probabilities C_0 and C_S for $S = 3$ modification sites and parameters $\lambda = \mu = 1$, $\beta = 3$ as a function of parameter α. We denote the stable steady states where $C_0 \approx 1$ (few PTMs) and $C_S \approx 1$ (large number of PTMs) by X and Z, respectively, and the unstable steady state by Y. For $\alpha \in [4.4, 7.5]$, steady states X, Y and Z appear, while for small α only X persists and for large α only Z persists.

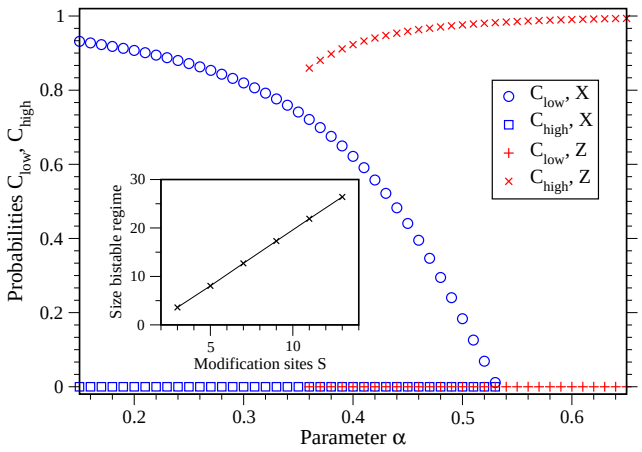

FIG. 3: Bifurcation diagram for $S = 50$ modification sites showing the steady state probabilities $C_{\rm low} = \sum_{n=0}^{4} C_n$ (i.e., low number of PTMs) and $C_{\rm high} = \sum_{n=46}^{50} C_n$ (i.e., high number of PTMs) of the stable steady states X and Z as a function of α. The remaining parameters are $\lambda = 5$, $\mu = 1$, $\beta = 0.01$. For $\alpha \in [0.36, 0.53]$, bistability persists. Note that $\alpha \ll \lambda$ and $\beta \ll \mu$. Inset: Width of the bistable regime in units of α as a function of the number of modification sites S ($\lambda = \mu = 1$, $\beta = 3$). It can be seen to increase linearly.

non-local feedback does not qualitatively affect the results of our study. We note that as long as one is interested in the asymptotics (asymptotically long time) behavior of solutions of difference equations, what matters as input in the equations is the ratio (relative strength) of various coupling parameters (e.g., β/α, λ/α, etc.). One can always divide by a non-zero coupling parameters and rescale time to absorb this parameter in the left-hand-side of the difference equations.

In section IV A, we will first discuss bistability in the model while neglecting spatial dependence. We will then incorporate spatial effects in part B, which we note fundamentally alters the picture. In section IV C, we discuss the effects of spatial heterogeneity and in section IV D, we discuss multiple correlated PTMs.

A. Multiple stable steady states in the S-state model and the role of S

In this section, we discuss the results of the nonlinear difference equations (10) when neglecting the spatial dependance, i.e., $C_{1,n} = C_{2,n} = ... = C_{N,n} = C_n$. In this case, a system of coupled nonlinear ordinary differential equations (ODE) is obtained,

$$\begin{aligned}
\frac{dC_0}{dt} &= -\lambda C_0 + \mu C_1 - 4\alpha C_0^2 + 4\beta C_0 C_1, \\
\frac{dC_n}{dt} &\overset{1\le n<S}{=} -\lambda(C_n - C_{n-1}) - \mu(nC_n - (n+1)C_{n+1}) - 4\alpha C_n(C_n - C_{n-1}) - 4\beta C_n(nC_n - (n+1)C_{n+1}), \\
\frac{dC_S}{dt} &= \lambda C_{S-1} - S\mu C_S + 4\alpha C_{S-1}C_S - 4S\beta C_S^2. \qquad (14)
\end{aligned}$$

Using this simplified ODE description, we evaluate steady states by setting $dC_n/dt = 0$, and study their stability by analyzing the Jacobian matrix. Expressions for the steady state probabilities C_n as a function of parameters λ, μ, α and β can be evaluated analytically. However, the resulting expressions are cumbersome and increasingly difficult to obtain for increasing S, and therefore calculations have been done numerically over a finite parameter range.

For more than one modification site, i.e., $S \geq 2$, and appropriately chosen parameters (see below) we find that a parameter regime exists where three steady states coexist. The multistability is a consequence of the nonlinearities

in Eqs.(14) that are introduced by the feedback terms. Two of the steady states are stable attractors and one steady state is an unstable saddle point. We note that no explicit cooperativity is required in order to obtain bistability if S is chosen larger or equal than two.

The bistability is illustrated in the bifurcation diagram of Fig. 2 where the steady state probabilities C_0 and C_3 are shown as a function of parameter α (the parameters used are $S = 3$, $\mu = \lambda = 1$, $\beta = 3$). If the feedback term for enzymes that catalyse the addition of PTMs is weak compared to the feedback term of enzymes that catalyse the removal of PTMs, only one steady state appears, as can be seen in Fig. 2 for $\alpha < 4.4$. This steady state, which we denote by X, is characterized by $C_0 \approx 1$, i.e., it corresponds to a state where very few PTMs are present. If the effects of the two terms that add PTMs approximately are roughly equal to the effects of the two terms that remove PTMs, three steady states exist ($\alpha \in [4.4, 7.5]$ in Fig. 2). In addition to steady state X, a steady state with $C_S \approx 1$ appears. This steady state corresponds to a state with a high number of PTMs, and we shall denote it by Z. A third steady state (denoted by Y in Fig. 2) is unstable. Finally, for large enough α, only steady state Z persists, as illustrated in Fig. 2 for $\alpha > 7.5$.

We note that in the previous paragraph we referred to the "strengths" of the four terms (1.-4. in section II) as they can be read from the expectation values, e.g., $\langle\Phi|\sum_i f(n_{i-1}, n_i, n_{i+1})|\Psi\rangle$. In contrast, in the following paragraph, we shall refer to the magnitudes of the coupling parameters (i.e., α, β, μ, λ) themselves. The values of the coupling parameters are controlled externally (e.g., the concentration, catalytic rate and diffusion rate of enzymes), while the expectation values also depend on system-dependent parameters (i.e., the number of modification sites S).

Bistability is obtained only if both feedback terms are present, i.e., if both α and β are non-zero. If the number of modification sites, S, is small, bistable steady states appear only if the coupling parameters of the feedback terms are large compared to those of the local terms, i.e., only if the ratios λ/α and μ/β are small enough. However, with increasing number of modification sites S, the size of the parameter regime where multiple steady states appear increases, as shown in the inset of Fig. 3, and for large enough S, bistability can be established even if $\alpha \ll \lambda$ and $\beta \ll \mu$, as shown in Fig. 3. The existence of a large number of modification sites S that are regulated by a particular set of enzymes thus allows for a larger parameter regime of bistability.

B. Spatial dependance

In this section we will explicitly take into account spatial dependence, which is incorporated in the solutions to equations (10). We numerically integrate (10) and find that the stable steady states that were discussed in the previous section may become unstable for certain initial conditions. We illustrate this in Fig. 4: We set the initial probabilities $C_{i,n}$ of the nucleosomes to those of steady state Z (the steady state where $C_{i,S}$ is large), except for very few nucleosomes where we set the initial probabilities to values close to those corresponding to the second steady state X [29]. It can be seen that the system approaches steady state X, i.e., the spatially restricted perturbation of the histone state causes instability. This instability manifests itself by traveling wave solutions of the system of equations (10). It can be seen in Fig. 4 that for a perturbation away from the boundaries, two traveling wave fronts develop which travel at a constant velocity towards the boundaries of the system. If the perturbation is located at one of the boundaries of the system, only one wave front develops.

There exists a set of parameters S, λ, μ, α and β where the velocity of the traveling wave(s) is zero. At that point, both steady states, X and Z, are stable with respect to spatial perturbations. For the parameters set of Fig. 4, this transition occurs at $\alpha^* \approx 5.7$ (bistability occurs for $\alpha \in [4.4, 7.5]$). For $\alpha < \alpha^*$ and within range of bistability, the steady state X is the "stronger attractor": If the initial state is Z and at least one nucleosome is perturbed such that its state is in the domain of fixed point X, the system approaches X, as is illustrated in Fig. 4. If the initial state is X, and at least one nucleosome is perturbed such that its state in the domain of steady state Z, the system bounces back into steady state X. In contrast, for $\alpha > \alpha^*$, steady state Z is the "stronger attractor": If the initial state is X and at least one nucleosome is perturbed such that its state is in the domain of Z, the system approaches Z. If the initial state is Z, and at least one nucleosome is perturbed such that its state is in the domain of attraction of X, the system bounces back into steady state Z.

In conclusion, for parameters $\alpha < \alpha^*$, steady state X exhibits a very high degree of stability as any initial state of the system that gives rise to traveling wave solutions yields traveling waves that drive the system into state X. In contrast, for parameters $\alpha > \alpha^*$, any traveling wave solution will drive the system into steady state Z. We note that when the asymptotic behaviour of equations (10) are considered, the number of nucleosomes in the system is not relevant. However, a larger number of nucleosomes does result in a longer duration for the traveling wave to spread over the entire system, which may be relevant if intermediate time scales are considered.

Instabilitities due to traveling wave solutions could have significant impact on the stability and inheritance of chromatin steady states in daughter cells upon division. During cell division, it is thought that the parental nucleosomes are randomly distributed among the two daughter cells, with the second half being newly synthesized [30].

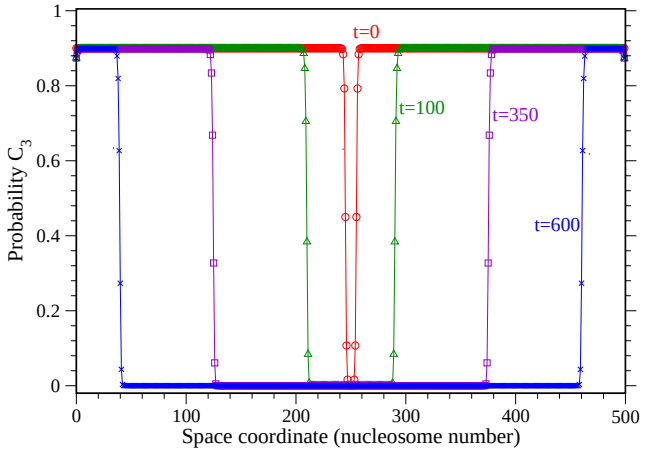

FIG. 4: Time evolution of probabilities $C_{i,3}(t)$. The system ($S = 3$ modification sites) is initially (time $t = 0$, red curve) in steady state Z (where $C_3 \approx 0.9$), except for few nucleosomes in the center that are strongly perturbed and whose probabilities are in the domain of steady state X. Parameters are $\lambda = \mu = 1$, $\beta = 3$, $\alpha = 5.6$. Two traveling wave fronts move towards the boundaries and drive the system into steady state X. The velocity of the waves is constant.

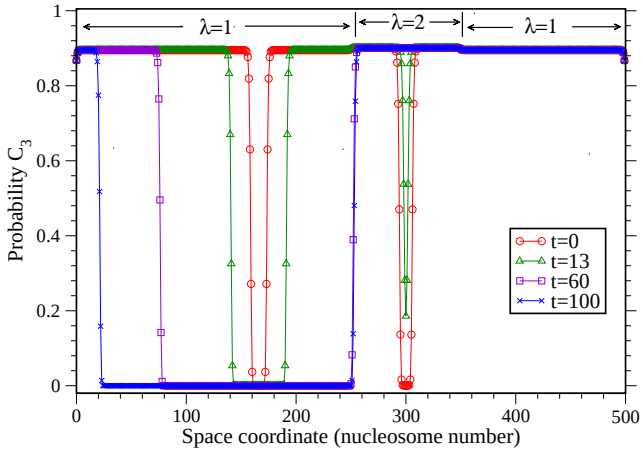

FIG. 5: Time evolution of probabilities $C_{i,3}(t)$. Parameters are as in Fig. 4, except that $\lambda = 1$ in part of the system, and $\lambda = 2$ in the remainder, as indicated. The system is initially in steady state Z except for few nucleosomes in both regions whose states lie in the domain of X (red circles). In the left region ($\lambda = 1$), two wave fronts move towards the boundaries, however, once the right front hits the $\lambda = 2$ region, it is stopped. In the $\lambda = 2$ region, the perturbation does not cause the system to approach X. The reason is that for $\lambda = 1$, steady state X is the "stronger attractor", while for $\lambda = 2$, Z is the "stronger attractor" (terminology see text).

The modification state of these new nucleosomes is crucial to the stability of the epigenetic state in the presence of non-local feedback terms. This can be seen as follows. The cell division can be modeled by replacing the states of half of the nucleosomes (randomly selected) at periodic intervals. Assume that the system is initially in steady state Z and parameters are set to the values of Fig. 4 where X is the "stronger attractor". If the states of the newly synthesized nucleosomes are random (i.e., any state is possible), some of these nucleosomes might be in states that are in the domain of steady state X right after cell division. In this case, a traveling wave can form, and drive the system into steady state X (after one, several or many divisions, depending on the time-scales involved). We have verified this numerically. However, if the states of the newly synthesized nucleosomes are correlated with the state of the nucleosomes in the mother cell such that the states of the new nucleosomes are in the domain of attraction of the original state, such instabilities cannot arise. In the presence of non-local effects, a sufficient correlation between mother and daughter nucleosome states is hence necessary to preserve the chromatin state. This would relate to the notion of epigenetic memory and in fact there is a relation between daugher cell state and mother state [an example was discussed in the second paragraph of the introduction]. However, how this is conveyed at the molecular level remains a challenging open question.

We conclude this section with a short discussion of the effects of considering explicit cooperative behaviour in the feedback terms. Explicit cooperative action of enzymes on-site, as well as of enzymes on nearest-neighbouring nucleosomes can be implemented using ansatz $f^{\rm coop}(n_{i-1}, n_i, n_{i+1}) = f(n_{i-1}, n_i, n_{i+1}) + \delta n_{i-1} n_i n_{i+1}$ and $g^{\rm coop}(n_{i-1}, n_i, n_{i+1}) = g(n_{i-1}, n_i, n_{i+1}) + \gamma(S - n_{i-1})(S - n_i)(S - n_{i+1})$ Using the approach of sections II, III and IV A, bistable steady states are observed, as was the case for the model without explicit cooperative action. However, bistability is possible even for the case $S = 1$. This in agreement with prior studies of two-state models with explicit cooperativity [15, 17]. The difference equations that are obtained using this ansatz, or their continuum version, admit traveling wave solutions, as in the case of our model without explicit cooperative behaviour (10) where $S \geq 2$.

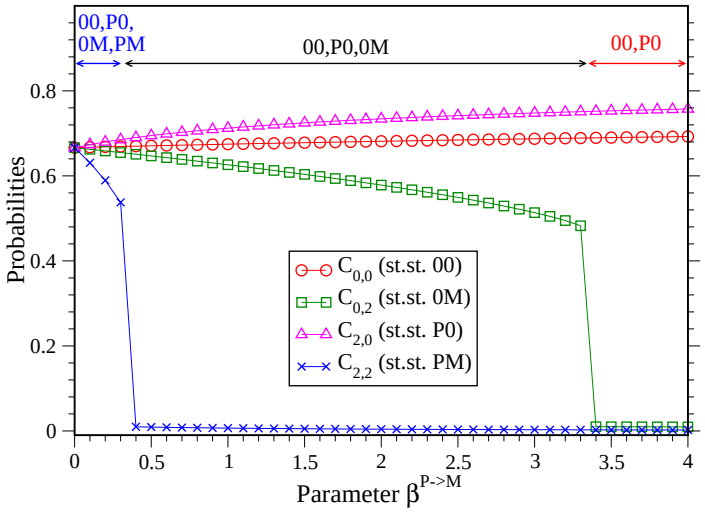

FIG. 6: Bifurcation diagram showing steady state probabilities $C_{p,m}$ of stable steady states for model (20) with two types of modifications, labeled by P and M, as a function of parameter $\beta^{P\to M}$. Note that only P inhibits M, but not vice versa, i.e., $\beta^{M\to P}=0$. The remaining parameters are given by $S^P=S^M=2$, $\lambda^P=\mu^P=\lambda^M=\mu^M=1$, $\beta^P=\beta^M=3$, $\alpha^P=\alpha^M=4.5$. For very small $\beta^{P\to M}$, four stable steady states (st.st.) exist, labeled by 00 (low P and low M), P0 (high P, low M), 0M (low P, high M), and PM (high P and high M). In an intermediate parameter regime, $\beta^{P\to M}\in[0.4,3.3]$, stable steady states 00, P0 and 0M persist, while for $\beta^{P\to M}>3.3$, only steady states 00 and P0 appear. We note that inhibition in only *one* direction (as $\beta^{M\to P}=0$) is sufficient to obtain a parameter regime where steady states have either a high number of PTMs P or M, or neither, but not both.

C. Spatially heterogeneous enzymatic activity

In biological systems, nucleosome modifying enzymes are typically recruited to specific regions of the chromatin by adaptor proteins, such as DNA-binding transcription factors. As a result, the activity of these enzymes depends on the region of the chromatin. The increased or decreased activity of enzymes at certain nucleosomes can be taken into account by including a spatial dependance in parameters λ and μ, i.e., λ_i and μ_i, where i is the nucleosome number. At each space point, the steady states are determined by the respective λ_i and μ_i, i.e., the steady states locally correspond to the steady states with homogenous activity. Hence the parameter regimes where multiple stable steady states appear vary in size and position, and steady state probabilities $C_{i,n}$ also depend on the nucleosome number i. For example, when choosing $S=3$, $\mu=1$, $\beta=3$, and $\lambda=1$, bistability exists for $\alpha\in[4.4,7.5]$ and $\alpha^*\approx 5.7$, while for parameters $S=3$, $\mu=1$, $\beta=3$ and $\lambda=2$, bistability persists for $\alpha\in[4.3,6.9]$, where $\alpha^*\approx 5.5$. As a consequence, for parameter $\alpha=5.6$, steady state X is the stronger attractor (in the sense explained in section IV B) for the former choice of parameters, while steady state Z is the stronger attractor for the latter choice of parameters. When perturbing a system that is initially in steady state Z in both λ-regions, traveling wave solutions drive the system into steady state X at the nucleosomes where $\lambda=1$, but not in regions where $\lambda=2$, and the traveling waves in the region where $\lambda=1$ are stopped once they hit regions where $\lambda=2$, as shown in Fig. 5. Spatial dependence on the activity of histone modifying enzymes that is conferred by recruitment to regulatory regions of chromatin by transcription factors may thus stabilize the histone state from local and non-local perturbation.

D. Multistability in model of several types of correlated PTMs

Most proteins, such as histones, that are subject to PTM-dependent regulation are regulated via multiple modifications. In this context, we discuss the results of including several types of modifications where each type is associated with different sets of enzymes, and thus different rate parameters λ, μ, α, β, $\tilde{\alpha}$ and $\tilde{\beta}$. For example, one might consider different classes of acetylation (or phosphorylation, ubiquitination, etc.) sites, each of them associated with a different enzyme. Alternatively, one might consider PTMs of type P (e.g., phosphorylation) and PTMs of type M

(e.g., methylation), with different rate parameters, λ^P and λ^M, α^P and α^M, etc. We denote by $C_{i,p,m}$ the probability of finding nucleosome i in the state with p PTMs of type P and m PTMs of type M. In this model, the number of stable steady states is four: the number of both M and P modifications is high (labeled by PM in the following), the number of P modifications is high and the number of M modifications is low (labeled by P0), the number of M modifications is high and the number of P modifications is low (labeled by 0M), and the number of both M and P modifications is low (labeled by 00). More generally, for T independent classes of modification sites, where a particular class of sites is associated with a particular set of coupling parameters, 2^T stable steady states are obtained. These steady states correspond to all possible combinations of states of high and low numbers of PTMs, i.e., all possible binary strings of length T.

In practice, however, different types and sites of PTMs are often not independent from each other. There are examples where the presence of a certain PTM inhibits the addition of another PTM. An example is the H3 N teminus where Ser10 phosphorylation inhibits Lys9 methylation [24]. In the following, we derive difference equations using the formalism introduced in sections II and III for a model of two types of PTMs, P and M, that mutually inhibit each other. We consider the processes 1.-4. (section II) separately for each of the two PTMs and add mutual inhibition (note that $m \equiv n^M$, $p \equiv n^P$):

$$n_i^P n_i^M \overset{\beta^{P\to M} n_i^P n_i^M}{\longrightarrow} n_i^P (n_i^M - 1), \tag{15}$$

$$n_i^P n_i^M \overset{\beta^{M\to P} n_i^P n_i^M}{\longrightarrow} (n_i^P - 1) n_i^M. \tag{16}$$

In the case of (15), the presence of PTMs of type P leads to the removal of PTMs of type M, and in the case of (16), the presence of PTMs of type M leads to the removal of PTMs of type P.

The wave function is of form (7) with the local wave functions given by

$$|\Psi_i(t)\rangle = \sum_{p=0}^{S^P} \sum_{m=0}^{S^M} C_{i,p,m}(t)|p\rangle|m\rangle \qquad \langle\Phi_i| = \sum_{p=0}^{S^P} \sum_{m=0}^{S^M} \langle p|\langle m|e^{\phi_{i,p,m}}, \tag{17}$$

where the normalization condition $\sum_{p=0}^{S^P}\sum_{m=0}^{S^M} C_{i,p,m} = 1$ applies. The local operators $\mathcal{R}_i$, $\mathcal{L}_i$, $\mathcal{N}_i$, $\mathcal{M}_i$, $\mathcal{I}_i$ are defined as in section III, and we denote the identity operator by $\mathcal{E}_i^X$ (unity matrix of size S^X). Using this notation, the "non-hermitian Hamiltonian" of the system is given by $\mathcal{H} = \sum_{i=1}^N \mathcal{H}_i$, where

$$\begin{aligned}
\mathcal{H}_i \;=\; & [\lambda^P + \alpha^P(\mathcal{N}_{i-1}^P + \mathcal{N}_{i+1}^P - 2\mathcal{N}_i^P) + \tilde{\alpha}^P \mathcal{N}_i^P](\mathcal{R}_i^P - \mathcal{I}_i^P)\mathcal{E}_i^M \\
& + \mathcal{E}_i^P[\lambda^M + \alpha^M(\mathcal{N}_{i-1}^M + \mathcal{N}_{i+1}^M - 2\mathcal{N}_i^M) + \tilde{\alpha}^M \mathcal{N}_i^M](\mathcal{R}_i^M - \mathcal{I}_i^M) \\
& + [\mu^P + \beta^P(\mathcal{M}_{i-1}^P + \mathcal{M}_{i+1}^P - 2\mathcal{M}_i^P) + \tilde{\beta}^P \mathcal{M}_i^P](\mathcal{L}_i^P - \mathcal{N}_i^P)\mathcal{E}_i^M \\
& + \mathcal{E}_i^P[\mu^M + \beta^M(\mathcal{M}_{i-1}^M + \mathcal{M}_{i+1}^M - 2\mathcal{M}_i^M) + \tilde{\beta}^M \mathcal{M}_i^M](\mathcal{L}_i^M - \mathcal{N}_i^M) \\
& + \beta^{P\to M}(\mathcal{L}_i^M - \mathcal{N}_i^M)\mathcal{N}_i^P + \beta^{M\to P}(\mathcal{L}_i^P - \mathcal{N}_i^P)\mathcal{N}_i^M.
\end{aligned} \tag{18}$$

The master equation in quantum variational formulation becomes

$$\left(\left\langle \frac{\partial \Phi}{\partial \phi_{i,p',m'}} \middle| \frac{\partial \Psi}{\partial C_{i,p,m}} \right\rangle \frac{dC_{i,p,m}}{dt} - \left\langle \frac{\partial \Phi}{\partial \phi_{i,p',m'}} |\mathcal{H}| \, \Psi \right\rangle \right)_{\phi_{i,p',m'=0}} = 0. \tag{19}$$

Evaluating (19) yields a system of nonlinear difference equations for the probabilities $C_{i,p,m}$ that the nucleosome at site i has p modifications of type P and m modifications of type M,

$$\begin{aligned}
\frac{dC_{i,p,m}}{dt} \;=\; & -(\lambda^P + \alpha^P F_i^{\nabla_P} + \tilde{\alpha}^P \langle n_i^P\rangle)(C_{i,p,m} - C_{i,p-1,m}) - (\lambda^M + \alpha^M F_i^{\nabla_M} + \tilde{\alpha}^M \langle n_i^M\rangle)(C_{i,p,m} - C_{i,p,m-1}) \\
& -(\mu^P + \beta^P G_i^{\nabla_P} + \tilde{\beta}^P \langle m_i^P\rangle)(pC_{i,p,m} - (p+1)C_{i,p+1,m}) - (\mu^M + \beta^M G_i^{\nabla_M} + \tilde{\beta}^M \langle m_i^M\rangle)(mC_{i,p,m} - (m+1)C_{i,p,m+1}) \\
& -\beta^{M\to P}\langle n_i^P\rangle(pC_{i,p,m} - (p+1)C_{i,p+1,m}) - \beta^{P\to M}\langle n^M\rangle(mC_{i,p,m} - (m+1)C_{i,p,m+1}).
\end{aligned} \tag{20}$$

Here $p = 0, 1, ..., S^P$, $m = 0, 1, ..., S^M$, and

$$F_i^{\nabla_X} = \langle n_{i-1}^X\rangle - 2\langle n_i^X\rangle + \langle n_{i+1}^X\rangle \quad \text{if} \quad 1 < i < N, \qquad F_1^{\nabla_X} = -2\langle n_1^X\rangle + \langle n_2^X\rangle \qquad F_N^{\nabla_X} = \langle n_{N-1}^X\rangle - 2\langle n_N^X\rangle,$$

$$G_i^{\nabla_X} = \langle m_{i-1}^X\rangle - 2\langle m_i^X\rangle + \langle m_{i+1}^X\rangle \quad \text{if} \quad 1 < i < N, \qquad G_1^{\nabla_X} = -2\langle m_1^X\rangle + \langle m_2^X\rangle \qquad G_N^{\nabla_X} = \langle m_{N-1}^X\rangle - 2\langle m_N^X\rangle,$$

where $X \in \{P, M\}$, and

$$\langle n_i^P \rangle = \sum_{p=0}^{S^P} \sum_{m=0}^{S^M} pC_{i,p,m}, \qquad \langle m_i^P \rangle = \sum_{p=0}^{S^P} \sum_{m=0}^{S^M} (S^P - p)C_{i,p,m} = S^P - \langle n_i^P \rangle,$$
$$\langle n_i^M \rangle = \sum_{p=0}^{S^P} \sum_{m=0}^{S^M} mC_{i,p,m},, \qquad \langle m_i^M \rangle = \sum_{p=0}^{S^P} \sum_{m=0}^{S^M} (S^M - m)C_{i,p,m} = S^M - \langle n_i^M \rangle.$$

In Eqs.(20), corrections for left-hand-side values of $p = 0$, $m = 0$, $p = S$, and $m = S$ have to be taken into account, similarly as in the first and third equation of (10).

We consider the case of inhibition in only one direction by setting $\beta^{M\to P} = 0$ and varying $\beta^{P\to M}$, as is the case in the example mentioned above where Ser10 phosphorylation inhibits Lys9 methylation. We evaluate steady states as explained in section (IV A). For parameter choices of $S^P = S^M = 2$, $\lambda^P = \mu^P = \lambda^M = \mu^M = 1$, $\beta^P = \beta^M = 3$, $\alpha^P = \alpha^M = 4.5$, $\tilde{\alpha}^P = 4\alpha^P$, $\tilde{\alpha}^M = 4\alpha^M$, $\tilde{\beta}^P = 4\beta^P$ and $\tilde{\beta}^M = 4\beta^M$, we observe that for small $\beta^{P\to M}$, all four stable steady states (as listed above) exist, as shown in Fig. 6. In an intermediate parameter regime only three stable steady states persist: 00, P0 and 0M, using the notation introduced above (Fig. 6). For large enough $\beta^{P\to M}$, only steady states 00 and P0 remain. This means that inhibitory interactions of two types of PTMs in only *one* direction are sufficient to obtain a parameter regime where steady states have either a high number of PTMs P or M, or neither, but not both. An analysis of traveling wave solutions of equations (20) similar to the one in section IV B applies in this case.

V. CONCLUSIONS AND OUTLOOK

The main results of this paper are as follows. We offer a robust method to obtain nonlinear partial differential equations describing the effective dynamics of histones. The method proceeds by mapping the system onto a quantum spin system whose dynamics is generated by a non-hermitian Hamiltonian. A feedback mechanism due to diffusion of enzymes along nucleosomes gives rise to multiple stable histone states. We study a number of novel aspects in histone systems that have not been reported before and are of biological relevance. We show that explicit cooperativity is not required to obtain multiple stable steady states as long as the number of PTMs is larger or equal to two, and we study the effects of varying the number of PTMs that are regulated by a particular set of enzymes. We also study the effect of spatially heterogeneous enzymatic on the histone state, and we apply our approach to a system of several correlated PTMs.

Our approach can easily be generalized to higher spatial dimensions and more complicated network topologies. Processes other than the ones considered in this work could be included into the master equation and other biological systems might be studied. In the context of post-translational histone modifications, it might be of interest to consider more complex and more realistic systems. For example, the particular structure of the core histones might be taken into account i.e., the exact arrangement of the different modifications on the different core histones. Feedback processes among different types of post-translational modifications might be considered, as well as feedback loops that arise due to interactions between the histones and the DNA in the chromatin. It also remains an open question to study the existence and stability of traveling wave solutions in the nonlinear reaction-diffusion equations that arise in our model from a mathematically rigorous point of view.

Acknowledgement.– We thank an anonymous referee for very helpful comments and suggestions that improved the presentation of the results in the paper.

[1] C.D. Allis, T. Jenuwein and T. Reinberg (Eds.). *Epigenetics*. Cold Spring Harbor Laboratory Press, Cold Spring Harbor (2007).
[2] C. Peterson and M. Laniel. Histones and histone modifications. *Current Biology* **14**, 546 (2004).
[3] O. J. Rando and H. Y. Chang. Genome-Wide Views of Chromatin Structure. *Annu. Rev. Biochem.* **78**, 245 (2009).
[4] S.I. Grewal and A.J. Klar. Chromosomal inheritance of epigenetic states in fission yeast during mitosis and meiosis. *Cell* **86**, 95 (1996).
[5] G. Thon and T. Friis. Epigenetic inheritance of transcriptional silencing and switching competence. *Genetics* **145**, 685 (1996).
[6] S.I. Grewal and S.C. Elgin. Heterochromatin: new possibilities for the inheritance of structure. *Curr. Opin. Genet. Dev.* **12**, 178 (2002).
[7] I.M. Hall *et.al.* Establishment and maintenance of a heterochromatin domain. *Science* **297**, 2232 (2002).
[8] B.M. Turner. Histone acetylation as an epigenetic determinant of long-term transcriptional competence. *Cell Mol. Life Sci.* **54**, 21 (1998).
[9] M. Grunstein. Yeast heterochromatin: regulation of its assembly and inheritance of histones. *Cell* **93**, 325 (1998).

[10] R.H. Jacobsen, A.G. Ladurner, D.S. King, and R. Tijan. Structure and function of a human TAFII250 double bromodomain module. *Science* **288**, 1422 (2000).

[11] D.J. Owen *et. al.* The structural basis for recognition of acetylated histone H4 by the bromodomain of histone acetyltransferase gcnp5. *EMBO J.* **19**, 6141 (2000).

[12] L.N. Rusche and J. Rine, Conversion of a gene-specific repressor to a regional silencer. *Genes Dev.* **15**, 955 (2001).

[13] G. Schotta *et. al.* Central role of Drosophila SU(VAR)3-9 in histone H3-K9 methylation and heterochromatic gene silencing. *EMBO J.* **21**, 1121 (2002).

[14] I.B. Dodd, M.A. Micheelsen, K. Sneppen and G. Thon. Theoretical analysis of epigenetic cell memory by nucleosome modification. *Cell* **129**, 813 (2007).

[15] M. Sedighi and A.M. Sengupta. Epigenetic chromatin silencing: bistability and front propagation. *Physical Biology* **4**, 246-255 (2003).

[16] In this work, we denote as mean-field description an effective continuum deterministic description (i.e., ordinary or partial differential equations). We obtain our mean-field Eqs. (11) by rescaling parameters in the difference equations (10) as explained, a procedure generally denoted as mean-field in the applied mathematics community.

[17] D. David-Rus, S. Mukhopadhyay, J.L. Lebowitz, and A.M. Sengupta. Inheritance of epigenetic chromatin silencing. *J. Theor. Biol.* **258**, 112 (2009).

[18] T. Jenuwein and C. D. Allis, Translating the histone code. *Science* **293**, 1074 (2001).

[19] D. Phanstiel, *et al.* Mass spectrometry identifies and quantifies 74 unique histone H4 isoforms in differentiating human embryonic stem cells. *Proc. Natl Acad. Sci. USA* **105**, 4093 (2008).

[20] J. J. Pesavento, *et. al.* Combinatorial modification of human histone H4 quantitated by two- dimensional liquid chromatography coupled with top down mass spectrometry. *J. Biol. Chem.* **283**, 14927 (2008).

[21] W.S. Lo *et.al.* Phosphorylation of serine 10 in histone H3 is functionally linked *in vitro* and *in vivo* to Gcn5-mediated acetylation at lysine 14. *Mol. Cell.* **5**, 917 (2000).

[22] Z.W. Sun and C.D. Allis. Ubiquitination of histone H2B regulates H3 methylation and gene silencing in yeast. *Nature* **418**, 104 (2002).

[23] H.H Ng, R.M. Xu, Y. Zhang, and K. Struhl. Ubiquitination of histone H2B by Rad6 is required for efficient Dot1-mediated methylation of histone H3 lysine79. *J. Biol. Chem.* **277**, 34655 (2002).

[24] S. Rea *et. al.* Regulation of chromatin structure by site-specific histone H3 methyltransferases. *Nature* **406**, 593 (2000).

[25] M. Doi. Second quantization representation for classical many-particle system. *J. Phys. A* **9**, 1465 (1976).

[26] L. Peliti. Path integral approach to birth-death processes on a lattice. *J. Phys. France* **46**, 1469 (1985).

[27] We note that the operators $\mathcal{R}$ and $\mathcal{L}$ do not correspond to bosonic creation and annihilation operators (bosonic commutation relations are not obeyed), but are the suitable operators for our model where S takes finite values.

[28] G.L. Eyink, Action principle in nonequilibrium statistical dynamics. *Phys. Rev. E* **54**, 3419 (1996).

[29] We choose $C_{i3}(t=0) = 0.5\bar{C}_3(2 - \tanh(i - N/2 + 5) + \tanh(i - N/2 - 5))$, where $\bar{C}_3 \approx 0.9$.

[30] A.T. Annunziato. Split decision: what happens to nucleosomes during DNA replication? *J. Biol. Chem.* **280**, 12065 (2005).